

# The nexus between disease surveillance, adaptive human behavior and epidemic containment

Baltazar Espinoza<sup>1\*†</sup>, Roger Sanchez<sup>2†</sup>, Jimmy Calvo-Monge<sup>3†</sup> Fabio Sanchez<sup>2†</sup>

<sup>1</sup>Biocomplexity Institute, University of Virginia, Virginia, USA.

<sup>2</sup>Escuela de Matemática-CIMPA, Universidad de Costa Rica, Ciudad Universitaria Rodrigo Facio, San José, 11501, Costa Rica.

<sup>3</sup>Centro de Investigación en Matemática Pura y Aplicada, Universidad de Costa Rica, Ciudad Universitaria Rodrigo Facio, San José, 11501, Costa Rica.

\*Baltazar Espinoza. Email: baltazar.espinoza@virginia.edu

†These authors contributed equally to this work.

**Epidemics exhibit interconnected processes that operate at multiple time and organizational scales—a hallmark of complex adaptive systems. Modern epidemiological modeling frameworks incorporate feedback between individual-level behavioral choices and centralized interventions. Nonetheless, the realistic operational course for disease detection, planning, and response is often overlooked. Disease detection is a dynamic challenge, shaped by the interplay between surveillance efforts and transmission characteristics. It serves as a tipping point that triggers emergency declarations, information dissemination, adaptive behavioral responses, and the deployment of public health interventions. Evaluating the impact of disease surveillance systems as triggers for adaptive behavior and public health interventions is key to designing effective control policies.**

**We examine the multiple behavioral and epidemiological dynamics gener-**

**ated by the feedback between disease surveillance and the intertwined dynamics of information and disease propagation. Specifically, we study the intertwined dynamics between: (i) disease surveillance triggering health emergency declarations, (ii) risk information dissemination producing decentralized behavioral responses, and (iii) centralized interventions. Our results show that robust surveillance systems that quickly detect a disease outbreak can trigger an early response from the population, leading to large epidemic sizes. The key result is that the response scenarios that minimize the final epidemic size are determined by the trade-off between the risk information dissemination and disease transmission, with the triggering effect of surveillance mediating this trade-off. Finally, our results confirm that behavioral adaptation can create a hysteresis-like effect on the final epidemic size.**

Epidemics exhibit interconnected processes that operate at multiple time and organizational scales, a hallmark of complex adaptive systems (1–3). The interdependency between human behavior and epidemics, influenced by endogenous feedback processes, is widely recognized. Together, behavioral-epidemiological dynamics generate a set of complexities shaping epidemic dynamics (4–10). At the individual level, transmission events are shaped by behaviors such as social interactions, mobility patterns, and interventions compliance (11–13). At the social level, factors like healthcare infrastructure, government policies, and socioeconomic conditions play crucial roles in shaping epidemic progression and management (14–16). Mathematical modeling has been effective in studying epidemic containment. There is an extensive literature of disease models incorporating distinct behavioral frameworks: threshold models of decision-making (17–21), game theory models of behavioral choices (22, 23), or behavioral choices based on cost-benefits trade-offs (24–28). However, the concurrent impacts of massive behavioral changes and the effects of interventions remain outstanding questions.

People do not passively comply with mandated interventions or suddenly change their behaviors. Information availability about the presence of a biological threat plays a key role in shaping the population’s responses (29–31). Awareness of infection risk and associated illness costs create cost-benefit trade-offs that drive behavioral adoption (15, 32). Moreover, declarations made by public health officials lead to alterations in people’s daily behavior over time, as knowledge and

understanding of the infection risk change. Consequently, preventive behaviors are typically adopted for a limited period, with potential relapses driven by pandemic fatigue and disease resurgence (8, 33, 34). Information dissemination and disease contagion are coupled antagonistic spreading processes as they exert opposing effects on individual behaviors (35). Each process exhibits its own dynamics, however, information spreading is inherently tied to the progression and detection of disease transmission.

Conventional models assume the population's innate ability to adopt preventive behaviors and implement interventions arbitrarily during an epidemic. The realistic operational course that accounts for disease detection, planning, and response is often overlooked. Disease surveillance systems are crucial for early warning, detection, and situational assessment of ongoing outbreaks. They provide valuable time to enhance our ability to respond to emerging biological threats (36–38). Disease detection is a dynamic challenge, shaped by the interplay between surveillance efforts and transmission characteristics. It serves as a tipping point that triggers emergency declarations, information dissemination, adaptive behavioral responses, and the deployment of public health interventions (39, 40). Incorporating the role of surveillance systems into mathematical modeling is critical to understanding the interdependence between epidemiological surveillance, disease dynamics and intervention strategies in an operational context.

We examine the multiple behavioral and epidemiological dynamics generated by the feedback between disease surveillance and the intertwined dynamics of information and disease propagation. In this work, we study the intertwined dynamics between: (i) disease surveillance triggering health emergency declarations, (ii) risk information dissemination producing decentralized behavioral responses, and (iii) centralized interventions. Our modeling framework focuses on a realistic course of action based on testing, analysis, and responses. We assume the epidemic originates within a naive population unaware of the ongoing disease outbreak. A health emergency triggers awareness dissemination upon disease detection, temporarily changing individuals' understanding of infection risk. This alters their behavior and turns them into risk communicators. We combine a probabilistic disease surveillance model with a behavioral-epidemiological model to analyze how the timing of health emergency declaration modulates behavioral responses and interventions, ultimately shaping epidemic outcomes. We let health emergency declarations alter disease transmission by triggering information dissemination, which modifies behavioral dynamics, and the timing of interventions.

Our modeling framework is schematically represented in Fig. 1. The SI Appendix provides a detailed formulation of the proposed modeling framework and a model extension incorporating awareness relapse. We focus on the final epidemic size as a key epidemiological metric for the impact of the disease and information transmission.

Our results shed light on the intrinsic relationship between the surveillance effort, the disease basic reproductive number, and the risk information transmission inducing behavioral responses. Specifically, we show that robust surveillance systems that quickly detect a disease outbreak can trigger an early response from the population, leading to high epidemic sizes under single-period responses (limited-duration behavioral adoption applied only once). In particular, the single-period most aggressive intervention is not always the best, commonly used strategy. The key result is that the response scenarios that minimize the final epidemic size are determined by the trade-off between the risk information dissemination and disease transmission, with the triggering effect of surveillance mediating this trade-off. On the other hand, our results align with previous findings that behavioral adaptation can create a hysteresis-like effect on the final epidemic size, a phenomenon not observed when only considering centralized interventions.

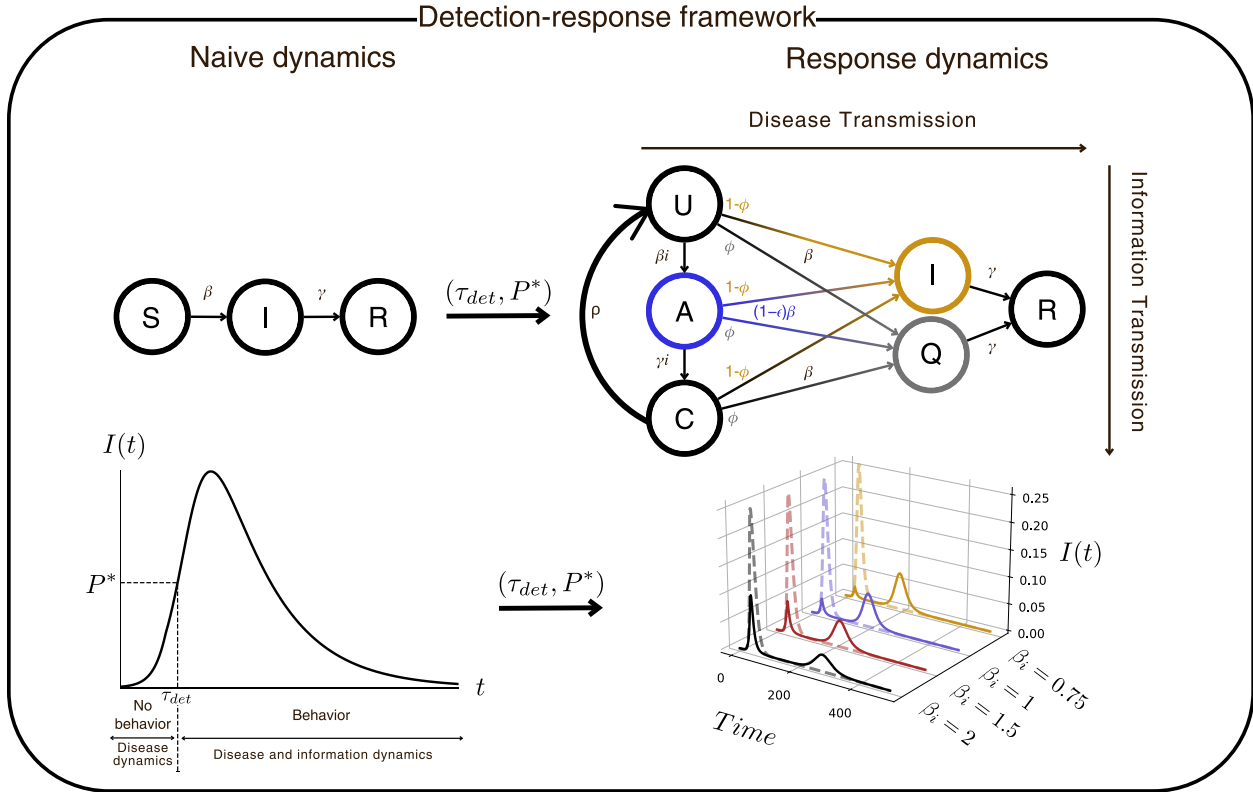


**Fig. 1: Schematic of our detection and response framework** Our framework captures the intertwined dynamics between disease dynamics spreading over a naive population, defining the detection time, and the disease dynamics produced by including behavior and interventions. The detection and response times depend on the surveillance effort and disease progression. This alters the contagion dynamics by triggering dueling dynamics between information dissemination and disease transmission, which ultimately shape the effects of behavior and interventions on the epidemiological outcomes.

## Disease surveillance triggers behavioral responses and interventions deployment

We begin by studying the impact of varying the disease basic reproductive number ( $\mathcal{R}_0^d$ ) on triggering information and behavioral dynamics and the final epidemic size. Fig. 2(A-C) illustrate the diverse disease dynamics the proposed framework produces. Specifically, Fig. 2A and B show the classical disease dynamics the proposed framework produces. Specifically, Fig. 2A and B show the classical scenarios where the epidemic dies out if  $\mathcal{R}_0^d < 1$ , and where the epidemic propagates when  $\mathcal{R}_0^d > 1$ ,

without detection and in the absence of behavioral responses. In contrast, Fig. 2C shows that highly infectious diseases trigger behavioral responses that significantly reduce the peak size and prolong the epidemic for a given disease prevalence threshold. Fig. 2D illustrates the impact of varying the disease transmission rate and infectious period on the final epidemic size. Our results identify three regions (denoted by dashed lines) where the epidemic progression exhibits distinct dynamics: (i) no epidemic propagation, where the epidemic dies out after onset ( $\mathcal{R}_0^d < 1$ ); (ii) intermediate final epidemic sizes, where the epidemic propagates, producing low enough prevalence levels to avoid detection ( $\mathcal{R}_0^d > 1$ ); and (iii) intermediate-high to high final epidemic sizes, where the epidemic reaches the detection threshold and triggers behavioral responses ( $\mathcal{R}_0^d \gg 1$ ).

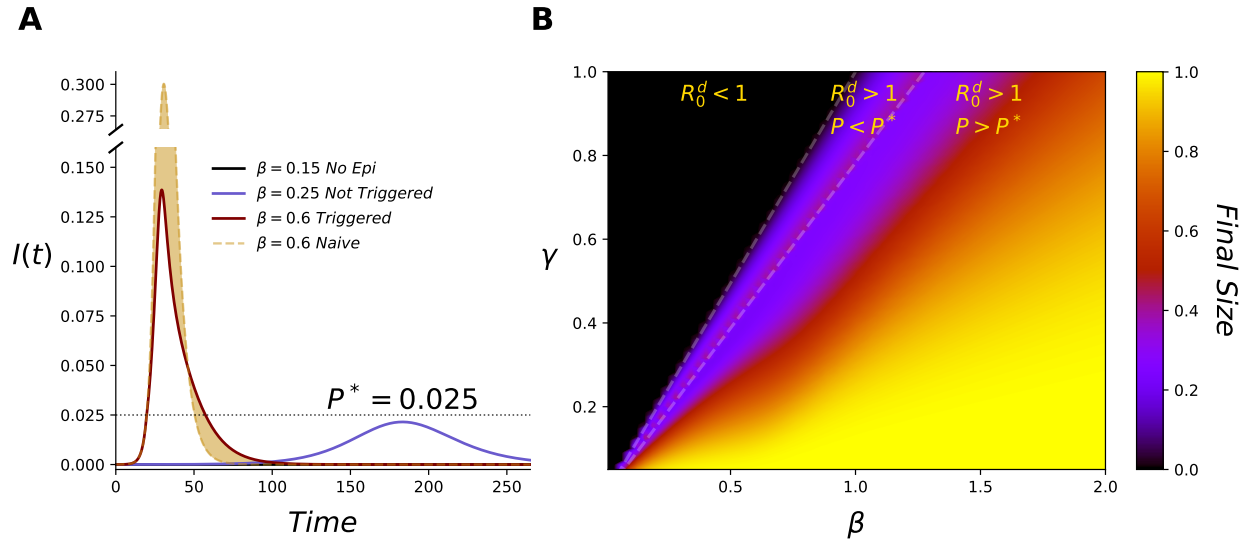


**Fig. 2: The impact of disease transmission characteristics on the behavior-disease dynamics and the final epidemic size. (A)** Time series of infectious individuals showing the potential dynamics produced by the proposed framework. We assume an average infectious period  $1/\gamma = 10$  days, and  $\mathcal{R}_0 = \{0.75, 1.25, 3\}$ , respectively. **(B)** Final epidemic sizes are attained by varying the disease infectiousness and period. We assume that the information dissemination exhibits a transmission likelihood of  $\beta_i = 1.5$ , and that aware individuals show an average response period of  $1/\gamma_i = 10$  days, during which their susceptibility reduces by a factor  $\epsilon = 0.8$ . We let the centralized response to quarantine a fraction  $\phi = 0.2$  of newly infected individuals and that surveillance effort triggers behavioral responses at a prevalence level of  $P^* = 0.025$ .

## Behavioral responses induce hysteresis in the final epidemic size

In this section, we examine the impact of the competing social and biological dynamics on the final epidemic size. Specifically, we show that for single-period interventions: (i) early responses do not minimize the final epidemic size, the impact of adaptive behavioral responses is influenced by the dynamics of risk information dissemination, where the final epidemic size exhibits a non-monotonic change as modifications in collective behavior accelerate; (ii) Hysteresis in the final epidemic size is driven by decentralized behavioral responses. Centralized interventions alone show a monotonic final epidemic size as a function of disease detection ( $P^*$ ), where behavioral response timing and stringency modulate the final size's non-monotonic change.

Hysteresis has previously been found in biological and social processes, such as drinking, where it was determined that the current state of drinkers depends on their previous state. In such a way that the susceptible-drinker and recovered-drinker flows contrast and help the drinking behavior developed (41).

We find that changes in the information dissemination rate ( $\beta_i$ ), mediate the timing of behavioral responses that produce a minimum on the final epidemic size. Our results in Fig. 3(A-B) show that behavioral responses triggered too soon produce large epidemics exhibiting reemergence dynamics. On the other hand, delayed behavioral responses are triggered at prevalence levels such that the final size is effectively reduced. However, if the behavioral responses are significantly delayed, the epidemic may have already reached a critical point to produce large outbreaks. Moreover, Fig. 3C shows that disease surveillance efforts influence the information dissemination rate minimizing the final epidemic size ( $P^*$ ). Our results highlight the impact of the intertwined nature of the dueling social and biological dynamics. We show that behavioral responses non-monotonically impact the final epidemic size, depending on the adoption rate of collective behavior and the disease detection time. Furthermore, the rapid dissemination of risk information can alleviate the lack of robust surveillance systems. In such scenarios, delayed disease detection is compensated by the swift spread of awareness.

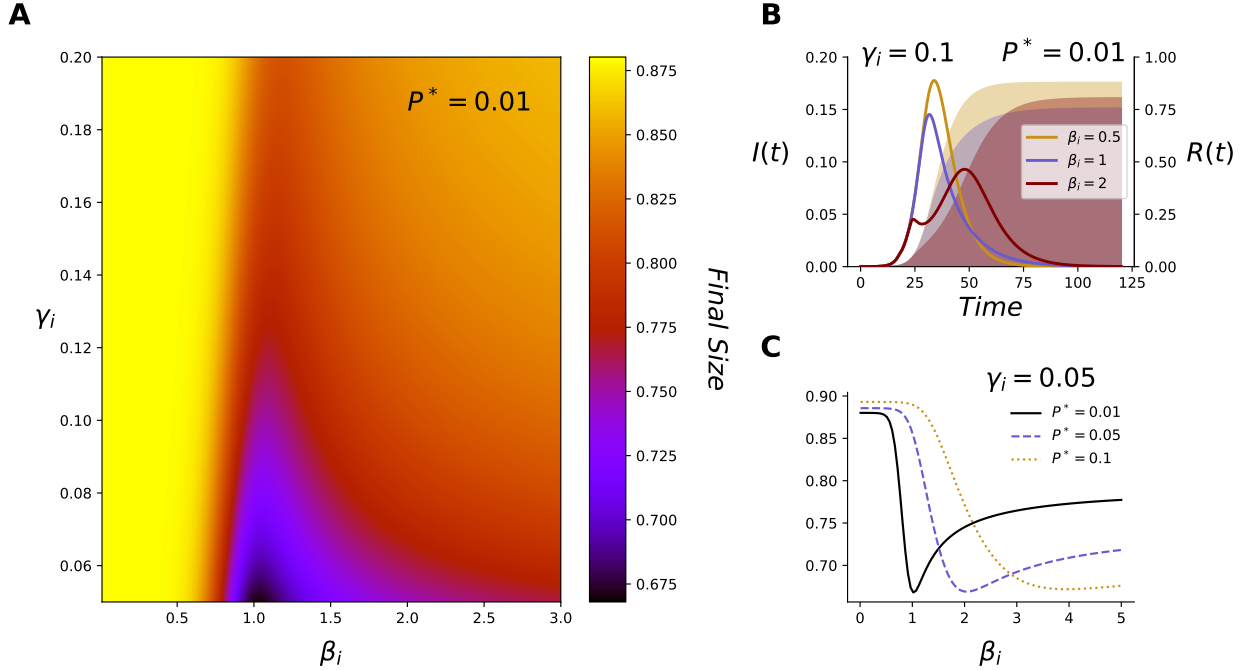


**Fig. 3: The impact of risk-information transmission characteristics on the final epidemic size.** (A) Final size as a function of the risk-information transmission rate ( $\beta_i$ ) and response withdrawal rate ( $\gamma_i$ ). Our results show that, regardless of the behavioral response withdrawal rate, the final size exhibits a non-monotonic reduction as the risk-information transmission rate increases. (B) Time series of infected and recovered subpopulations for distinct risk-information transmission rates ( $\beta_i = 0.5, 1, 2$ ), and response withdrawal rate  $\gamma_i$  of 10 days. (C) Final size as a function of the information transmission rate, for surveillance efforts leading disease detection at  $P^* = 0.01$ ,  $P^* = 0.05$ , and  $P^* = 0.1$ . Early disease detection scenarios show a sharp minimum as a function of information transmission rate. Delayed disease detection requires higher information transmission rates and shows broader minimums.

The intuition behind the non-linear impact of information dissemination on the final epidemic size is represented in Fig. 3B. We show selected time series of the infected and recovered subpopulations, for  $\beta_i$  values that produce distinct behavioral-disease dynamics. The risk-information dissemination rate producing the lowest number of recovered individuals corresponds to the intermediate value. Moreover, lower (greater)  $\beta_i$  values generate a very delayed (a very early) behavioral response, producing a minimal impact on the epidemic size.

We next explore the effects of decentralized adaptive behavioral responses of aware individuals

( $\epsilon$ ) and centralized intervention quarantining a fraction of the newly infected individuals ( $\phi$ ), for distinct disease surveillance efforts ( $P^*$ ). Fig. 4(A-C) show that while both centralized and decentralized responses decrease the final epidemic size, non-monotonic changes are exhibited only in the presence of adaptive behavioral responses. As behavioral efforts decrease ( $\epsilon = 0$ ), the final epidemic size shows monotonic increments. However, as behavioral responses become more prominent, the final epidemic size exhibits non-monotonic increments. Furthermore, our results in Fig. 4(D-F) show that the non-monotonic effect on the final size exhibits limited sensitivity to changes in quarantine capacity. While increases in quarantine capacity amplify the impact of behavioral responses on reducing the disease burden, this does not affect the trade-off between surveillance and behavioral responses. In these scenarios, delayed disease detection combined with strong behavioral responses minimizes the final epidemic size.

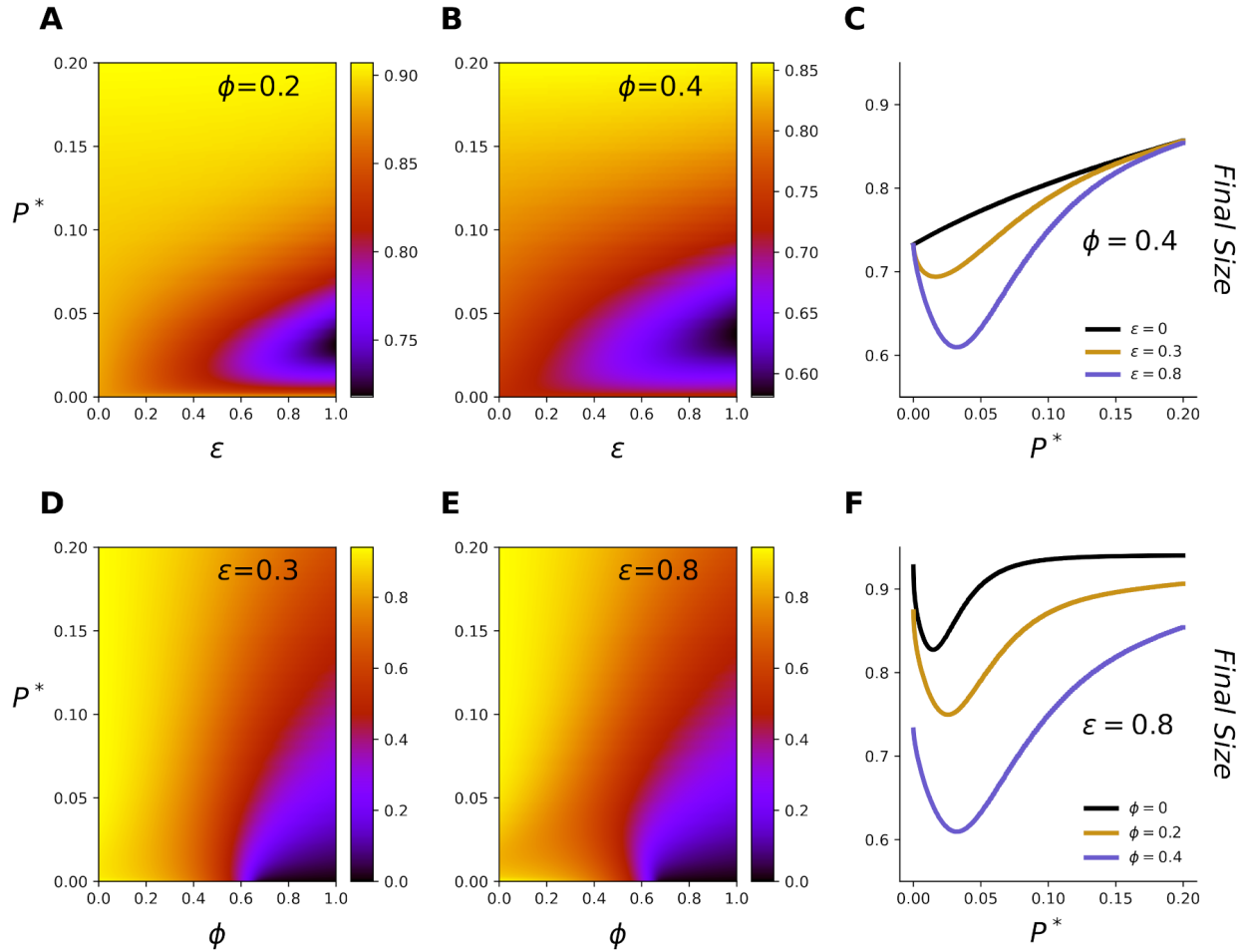


**Fig. 4: The trade-off between centralized interventions and adaptive behavior, on the final epidemic size. (A and B)** Final epidemic sizes as a function of the behavioral response stringency ( $\epsilon$ ) and the surveillance efforts ( $P^*$ ), for quarantine capacities of  $\phi = 0.2$  and  $\phi = 0.4$ . Our results show non-monotonic changes on the final epidemic size as the surveillance effort decreases. **(C)** The local minimum emerges and is exacerbated by increments on the behavioral response stringency. **(D and E)** Final epidemic sizes as a function of quarantine capacity ( $\phi$ ) and surveillance efforts ( $P^*$ ), for behavioral response stringency of  $\epsilon = 0.3$  and  $\epsilon = 0.3$ . Low stringency of behavioral responses ( $\epsilon = 0.3$ ) vanishes the non-monotonic changes on the final epidemic size. High stringency of behavioral responses ( $\epsilon = 0.8$ ) exhibit non-monotonic changes on the final epidemic size regardless of the quarantine capacity.

## Conclusion

Disease surveillance systems offer early warnings of outbreaks before they escalate into public health emergencies. The detection of biological threats represents trigger events that start a variety of signaling cascades that activate multiple responses. The dissemination of an alert status during epidemics often exhibits transmission dynamics independent of the disease progression, and can show multiple transmission dynamics (29, 30, 38, 42). Social media and news, or mouth-to-mouth information dissemination, could cause massive awareness, potentially leading to collective changes in individuals' behaviors. In this work, we assume that the implementation of epidemic interventions and the adoption of risk-avoidance behaviors are preceded by identifying a biological threat. Our coupled disease surveillance model serves as an operational tipping point for public health authorities and the population's spread of awareness leading to preventive behaviors.

Our results highlight the role of disease surveillance as a trigger for public health interventions and adaptive human behavior, emphasizing the complex feedback mechanisms that shape the dueling dynamics of disease progression and risk awareness. We showed that surveillance efforts, by influencing the timing of emergency declarations and triggering risk communication and behavioral responses, significantly affect the final size of the epidemic. Moreover, our findings underscore the importance of surveillance systems in modulating the effectiveness of interventions to mitigate the impact of epidemics. Rapid detection of biological threats enhances public awareness, prompting early behavioral changes and the implementation of intervention strategies. However, our results reveal that the timing of behavioral adoption is critical, as both early and delayed responses can lead to suboptimal outcomes. In particular, we identify a trade-off between risk information dissemination and disease transmission dynamics, where an overly aggressive early response may not always result in the smallest epidemic size. This result is crucial for strategic planning in determining the optimal timing for triggering behavioral responses and interventions. Furthermore, our analysis illustrates how decentralized behavioral adaptations, influenced by social awareness and information spread, can create hysteresis-like effects on the final epidemic size. The emergence and modulation of this phenomenon in the presence of behavioral responses suggests that the effectiveness of public health policies heavily depends on the dynamic interplay between individual decision-making and collective responses. Our results align with existing literature showing that

individual-specific control measures outperform population-wide measures (17, 21, 43, 44).

Our extended model, incorporating awareness relapse, provides further insights into the dynamics of epidemic control. The potential for individuals to revert to pre-awareness behaviors suggests that sustained public health messaging and reinforcement strategies are necessary to prevent a resurgence of disease transmission. Additionally, our results align with previous studies indicating that effective disease containment requires balancing top-down intervention policies and bottom-up behavioral responses (15, 36, 45). Finally, this work provides a quantitative framework for understanding the interplay between disease surveillance, public health decision-making, and the joint dynamics of adaptive human behavior and epidemics. The insights gained from this study aim to inform the design of effective epidemic containment strategies by optimizing the timing of emergency declarations, integrating the impact of risk communication, and accounting for the dynamics of behavioral responses to minimize the societal burden of infectious diseases.

## References and Notes

1. S. Levin, Complex adaptive systems: exploring the known, the unknown and the unknowable. *Bulletin of the American mathematical Society* **40** (1), 3–19 (2003).
2. S. A. Levin, The problem of pattern and scale in ecology: the Robert H. MacArthur award lecture. *Ecology* **73** (6), 1943–1967 (1992).
3. J. Liu, *et al.*, Complexity of coupled human and natural systems. *science* **317** (5844), 1513–1516 (2007).
4. J. J. V. Bavel, *et al.*, Using social and behavioural science to support COVID-19 pandemic response. *Nature human behaviour* **4** (5), 460–471 (2020).
5. H. Seale, *et al.*, COVID-19 is rapidly changing: Examining public perceptions and behaviors in response to this evolving pandemic. *PloS one* **15** (6), e0235112 (2020).
6. C. Moya, *et al.*, Dynamics of behavior change in the COVID world. *American Journal of Human Biology* (2020).
7. S. Pagliaro, *et al.*, Trust predicts COVID-19 prescribed and discretionary behavioral intentions in 23 countries. *PloS one* **16** (3), e0248334 (2021).
8. A. Petherick, *et al.*, A worldwide assessment of changes in adherence to COVID-19 protective behaviours and hypothesized pandemic fatigue. *Nature Human Behaviour* **5** (9), 1145–1160 (2021).
9. J. Chen, A. Marathe, M. Marathe, Feedback between behavioral adaptations and disease dynamics. *Scientific reports* **8** (1), 12452 (2018).
10. J. J. Van Bavel, *et al.*, Using social and behavioural science to support COVID-19 pandemic response. *Nature human behaviour* **4** (5), 460–471 (2020).
11. M. Chinazzi, *et al.*, The effect of travel restrictions on the spread of the 2019 novel coronavirus (COVID-19) outbreak. *Science* **368** (6489), 395–400 (2020).

12. B. Espinoza, C. Castillo-Chavez, C. Perrings, Mobility restrictions for the control of epidemics: When do they work? *Plos one* **15** (7), e0235731 (2020).
13. S. Chang, *et al.*, Mobility network models of COVID-19 explain inequities and inform reopening. *Nature* **589** (7840), 82–87 (2021).
14. P. Klepac, R. Laxminarayan, B. T. Grenfell, Synthesizing epidemiological and economic optima for control of immunizing infections. *Proceedings of the National Academy of Sciences* **108** (34), 14366–14370 (2011).
15. A. Glaubitz, F. Fu, Social dilemma of nonpharmaceutical interventions: Determinants of dynamic compliance and behavioral shifts. *Proceedings of the National Academy of Sciences* **121** (50), e2407308121 (2024).
16. C. M. Saad-Roy, A. Traulsen, Dynamics in a behavioral–epidemiological model for individual adherence to a nonpharmaceutical intervention. *Proceedings of the National Academy of Sciences* **120** (44), e2311584120 (2023).
17. Z. Qiu, *et al.*, Understanding the coevolution of mask wearing and epidemics: A network perspective. *Proceedings of the National Academy of Sciences* **119** (26), e2123355119 (2022).
18. M. Granovetter, Threshold models of collective behavior. *American journal of sociology* **83** (6), 1420–1443 (1978).
19. D. Guilbeault, J. Becker, D. Centola, Complex contagions: A decade in review. *Complex spreading phenomena in social systems: Influence and contagion in real-world social networks* pp. 3–25 (2018).
20. P. S. Dodds, D. J. Watts, A generalized model of social and biological contagion. *Journal of theoretical biology* **232** (4), 587–604 (2005).
21. B. Morsky, F. Magpantay, T. Day, E. Akçay, The impact of threshold decision mechanisms of collective behavior on disease spread. *Proceedings of the National Academy of Sciences* **120** (19), e2221479120 (2023).

22. T. C. Reluga, Game theory of social distancing in response to an epidemic. *PLoS computational biology* **6** (5), e1000793 (2010).
23. C. T. Bauch, D. J. Earn, Vaccination and the theory of games. *Proceedings of the National Academy of Sciences* **101** (36), 13391–13394 (2004).
24. B. Espinoza, M. Marathe, S. Swarup, M. Thakur, Asymptomatic individuals can increase the final epidemic size under adaptive human behavior. *Scientific reports* **11** (1), 19744 (2021).
25. B. Espinoza, S. Swarup, C. L. Barrett, M. Marathe, Heterogeneous adaptive behavioral responses may increase epidemic burden. *Scientific Reports* **12** (1), 11276 (2022).
26. B. Espinoza, *et al.*, The impact of risk compensation adaptive behavior on the final epidemic size. *Mathematical Biosciences* p. 109370 (2025).
27. C. Perrings, *et al.*, Merging economics and epidemiology to improve the prediction and management of infectious disease. *EcoHealth* **11** (4), 464–475 (2014).
28. E. P. Fenichel, *et al.*, Adaptive human behavior in epidemiological models. *Proceedings of the National Academy of Sciences* **108** (15), 6306–6311 (2011).
29. S. Funk, E. Gilad, C. Watkins, V. A. Jansen, The spread of awareness and its impact on epidemic outbreaks. *Proceedings of the National Academy of Sciences* **106** (16), 6872–6877 (2009).
30. S. Towers, *et al.*, Mass media and the contagion of fear: the case of Ebola in America. *PloS one* **10** (6), e0129179 (2015).
31. M. Schaller, The behavioural immune system and the psychology of human sociality. *Philosophical Transactions of the Royal Society B: Biological Sciences* **366** (1583), 3418–3426 (2011).
32. X. Chen, F. Fu, Imperfect vaccine and hysteresis. *Proceedings of the royal society B* **286** (1894), 20182406 (2019).
33. J. Bosman, S. Mervosh, M. Santora, As the Coronavirus Surges, a New Culprit Emerges: pandemic Fatigue. *New York Times* (2020), <https://www.nytimes.com/2020/10/17/us/>

coronavirus-pandemic-fatigue.html, <https://www.nytimes.com/2020/10/17/us/coronavirus-pandemic-fatigue.html>.

34. M. Santora, I. Kwai, As Virus Surges in Europe, Resistance to New Restrictions Also Grows. *New York Times* (2020), <https://www.nytimes.com/2020/10/09/world/europe/coronavirus-europe-fatigue.html>, <https://www.nytimes.com/2020/10/09/world/europe/coronavirus-europe-fatigue.html>.
35. M. De Domenico, C. Granell, M. A. Porter, A. Arenas, The physics of spreading processes in multilayer networks. *Nature Physics* **12** (10), 901–906 (2016).
36. B. Espinoza, *et al.*, Coupled models of genomic surveillance and evolving pandemics with applications for timely public health interventions. *Proceedings of the National Academy of Sciences* **120** (48), e2305227120 (2023).
37. C. Chen, *et al.*, Wastewater-based epidemiology for covid-19 surveillance: A survey. *ArXiv* (2024).
38. K. J. Margevicius, *et al.*, The Biosurveillance Analytics Resource Directory (BARD): facilitating the use of epidemiological models for infectious disease surveillance. *PLoS One* **11** (1), e0146600 (2016).
39. H. N. Perry, *et al.*, Planning an integrated disease surveillance and response system: a matrix of skills and activities. *BMC medicine* **5**, 1–8 (2007).
40. C. M. Wolfe, *et al.*, Systematic review of Integrated Disease Surveillance and Response (IDSR) implementation in the African region. *PLoS One* **16** (2), e0245457 (2021).
41. F. Sánchez, X. Wang, C. Castillo-Chávez, D. M. Gorman, P. J. Gruenewald, Drinking as an epidemic—a simple mathematical model with recovery and relapse, in *Therapist’s Guide to Evidence-Based Relapse Prevention* (Elsevier), pp. 353–368 (2007).
42. S. Funk, E. Gilad, V. Jansen, Endemic disease, awareness, and local behavioural response. *Journal of theoretical biology* **264** (2), 501–509 (2010).

43. J. O. Lloyd-Smith, S. J. Schreiber, P. E. Kopp, W. M. Getz, Superspreading and the effect of individual variation on disease emergence. *Nature* **438** (7066), 355–359 (2005).
44. M. S. Mahmud, S. Eshun, B. Espinoza, C. Kadelka, Adaptive human behavior and delays in information availability autonomously modulate epidemic waves. *medRxiv* pp. 2024–11 (2024).
45. A. K. Dixit, B. Espinoza, Z. Qiu, A. Vullikanti, M. V. Marathe, Airborne disease transmission during indoor gatherings over multiple time scales: Modeling framework and policy implications. *Proceedings of the National Academy of Sciences* **120** (16), e2216948120 (2023).

## Acknowledgments

### Supplementary materials

Materials and Methods

Supplementary Text

Figs. S1 to S9

References (7-45)

**Supplementary Materials for**  
**The nexus between disease surveillance, adaptive human**  
**behavior and epidemic containment**

Baltazar Espinoza<sup>1\*†</sup>, Roger Sanchez<sup>2†</sup>, Jimmy Calvo-Monge<sup>3†</sup> Fabio Sanchez<sup>2†</sup>

\*Baltazar Espinoza. Email: be8dq@virginia.edu

†These authors contributed equally to this work.

**This PDF file includes:**

Materials and Methods

Supplementary Text

Figures S1 to S9

## Materials and Methods

### Coupling disease surveillance and epidemic dynamics

Our coupled behavioral-epidemiological model depicted in Figure 1 assumes the epidemic initially spreads among a naive population with a Susceptible-Infected-recovered scheme formalized by equation (S1)

$$\begin{aligned}\dot{S} &= -\beta S \frac{I}{N}, \\ \dot{I} &= \beta S \frac{I}{N} - \gamma I, \\ \dot{R} &= \gamma I,\end{aligned}\tag{S1}$$

where  $\beta$  corresponds to the transmission rate, and  $\gamma$  is the recovery rate. We couple the disease progression model with a surveillance model formulated using a probabilistic approach to compute the expected time required to identify at least a single infected individual using power calculations. Assuming a homogeneous mixing population and a random sampling strategy, we compute the cumulative probability of detecting at least one infectious individual. The proposed disease detection model incorporates the dynamic progression of the epidemic into the daily probability of detecting infectious individuals. The probability of detecting at least a single positive case by time  $t$ , for a disease prevalence level of  $\phi_s$  on day  $s$ , for surveillance effort of  $N_s$  daily tested individuals, is given by

$$\mathbb{P}_{det} = 1 - \prod_{s=1}^t (1 - \phi_s)^{N_s}.\tag{S2}$$

Finally, we let the disease detection time ( $\tau_{det}$ ) to be reached at the time at least a single infectious individual is detected with at least 95% confidence,  $\mathbb{P}_{det} = 0.95$ . The detection time determines the disease prevalence threshold ( $P^*$ ) at which health emergency declarations are issued. Note that  $P^*$  is not arbitrarily selected; instead it depends on the preselected surveillance effort.

### Disease surveillance triggers interventions, risk information spread and adaptive human behavior

Upon health emergency declaration, we assume the onset of centralized intervention quarantining a fraction  $\phi$  newly infected individuals ( $Q$ ), and that the susceptible population is divided into the

following subgroups based on their knowledge about the epidemic: Unaware ( $U$ ), who are naive of the infection risk; Aware ( $A$ ), who are informed of the infection risk, adopt preventive behaviors, and are ready to convey information; and Careless ( $C$ ), who are informed of the infection risk but do not adopt preventive behaviors or convey information. Dissemination of awareness (information about infection risk) begins with a single aware individual conveying the information to unaware individuals at a transmission rate  $\beta_i$ . Aware individuals adopt preventive behaviors that reduce their susceptibility to disease transmission by a factor of  $(1 - \epsilon)$  during an average period of  $1/\gamma$  days. After this period, individuals become careless and stop adopting preventive behaviors, exhibiting the same susceptibility to disease transmission as unaware individuals. Moreover, we assume the health emergency declaration triggers quarantine as a mandated intervention. Regardless of their knowledge status, a fraction  $\phi$  of the newly infected individuals are quarantined until recovery, during which they cannot transmit the disease. The dynamics as mentioned above are formalized by the set of differential equations in Equation (S3)

$$\begin{aligned}
\dot{U} &= -\beta_i U \frac{A}{N} - \beta U \frac{I}{N}, \\
\dot{A} &= \beta_i U \frac{A}{N} - (1 - \epsilon) \beta A \frac{I}{N} - \gamma_i A, \\
\dot{C} &= \gamma_i A - \beta C \frac{I}{N}, \\
\dot{Q} &= \phi \beta [U + C + (1 - \epsilon) A] \frac{I}{N} - \gamma Q, \\
\dot{I} &= (1 - \phi) \beta [U + C + (1 - \epsilon) A] \frac{I}{N} - \gamma I, \\
\dot{R} &= \gamma(Q + I),
\end{aligned} \tag{S3}$$

where  $\epsilon$  represents the stringency of the behavioral response,  $\phi$  denotes the proportion of quarantined individuals,  $\beta_i$  is the information transmission rate,  $\gamma_i$  correspond to the information transmission and recovery rates, and  $\beta$  and  $\gamma$  are the disease transmission and recovery rate, respectively.

### **Adaptive behavior relapse model**

We extend the model (S3) by incorporating a potential relapse of careless individuals that allows for multiple adoption cycles of precautionary behavior. We assume that a careless individual ( $C$ ) loses interest in the epidemic progression and returns to unaware status ( $U$ ) at a rate  $\rho$ , after which it could become aware again by interacting with aware individuals. The dynamics mentioned above

are represented in model (S4)

$$\begin{aligned}
\dot{U} &= -\beta_i U \frac{A}{N} - \beta U \frac{I}{N} + \rho C, \\
\dot{A} &= \beta_i U \frac{A}{N} - (1 - \epsilon) \beta A \frac{I}{N} - \gamma_i A, \\
\dot{C} &= \gamma_i A - \beta C \frac{I}{N} - \rho C, \\
\dot{Q} &= \phi \beta [U + C + (1 - \epsilon) A] \frac{I}{N} - \gamma Q, \\
\dot{I} &= (1 - \phi) \beta [U + C + (1 - \epsilon) A] \frac{I}{N} - \gamma I, \\
\dot{R} &= \gamma (Q + I).
\end{aligned} \tag{S4}$$

## Scenario robustness

In this section, we explore the robustness of our results as a function of distinct disease and information scenarios. Specifically, we study the impact of varying the length of the infectious and behavior periods and disease and information transmission likelihood on modulating the final epidemic size.

### Single period behavioral response scenario

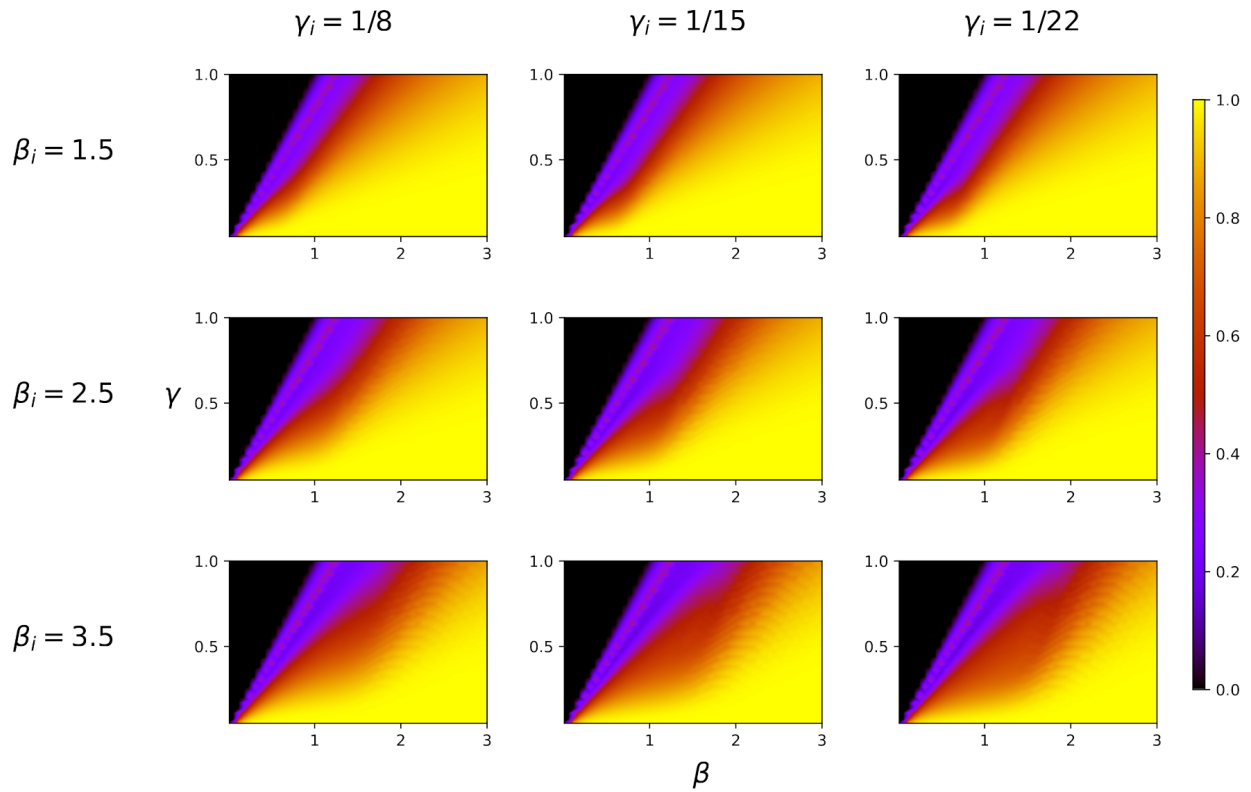


**Fig. S1: Grid of informative parameters comparison.** Shows the gradual change when different infection and recovery rates are set in the informative section of the model, providing an idea of the 4-dimensional motion presented through the model's sensitivity. The grid is composed by the sets of  $\beta_i \in \{1.5, 2.5, 3.5\}$  and  $\gamma_i \in \{1/8, 1/15, 1/22\}$ ; while the other parameters are considered fixed.

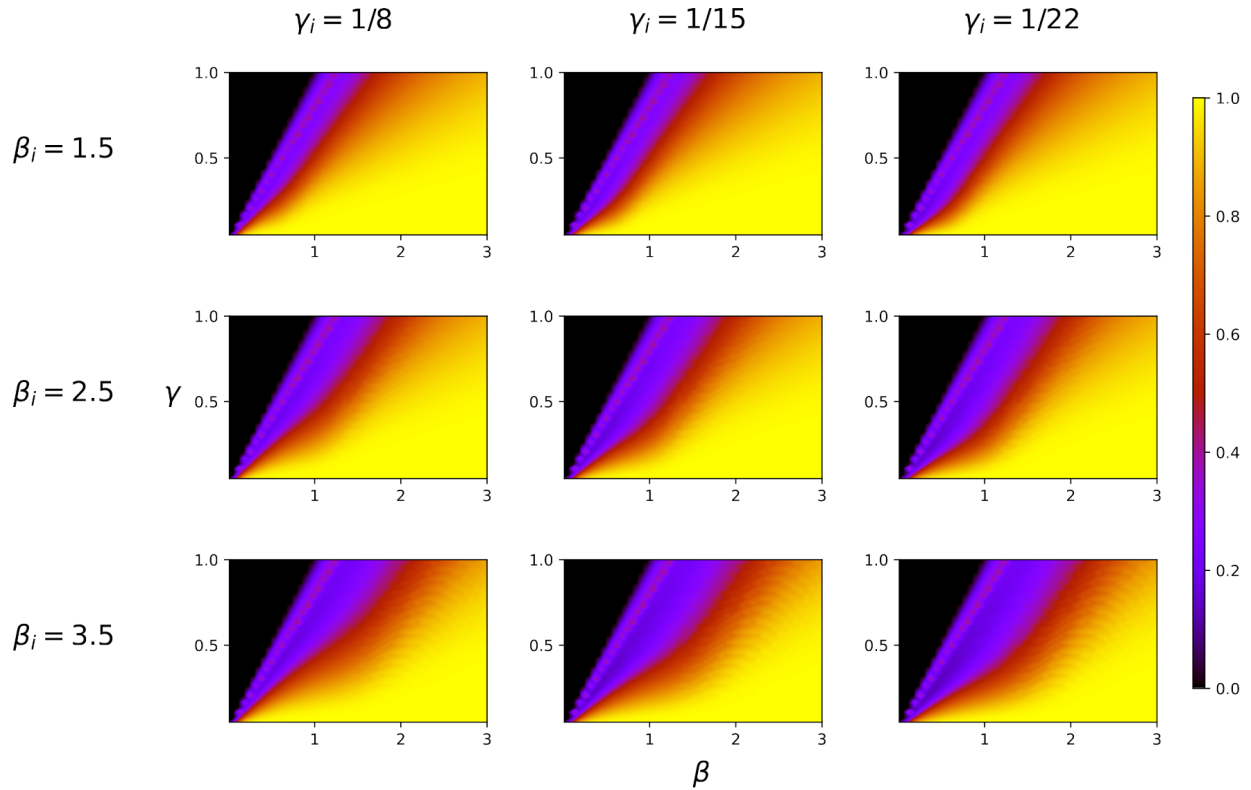


**Fig. S2: Grid of informative parameters comparison in a multiple shot framework.** Shows the gradual change when different infection and recovery rates are set in the informative section of the model, providing an idea of the 4-dimensional motion presented through the model's sensitivity. The grid is composed by the sets of  $\beta_i \in \{1.5, 2.5, 3.5\}$  and  $\gamma_i \in \{1/8, 1/15, 1/22\}$ ; while the other parameters are considered fixed with  $\rho = 1/20$ .

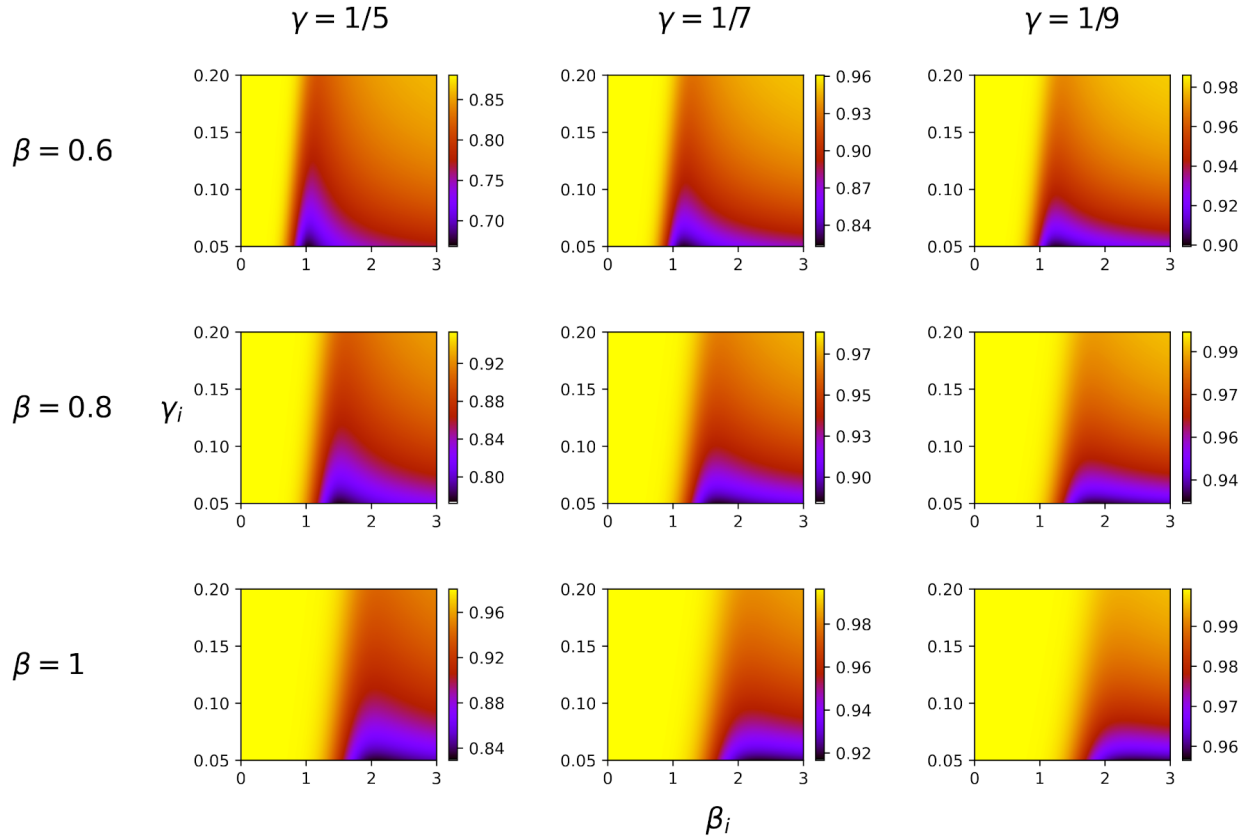


**Fig. S3: Grid of infectious parameters comparison.** Shows the gradual change when different infectious and recovery rates are set in the infectious section of the model. Each subplot has its color bar showing the distribution of values. The grid is composed by the sets of  $\beta \in \{0.6, 0.8, 1\}$  and  $\gamma \in \{1/5, 1/7, 1/9\}$ ; while the other parameters are considered fixed.

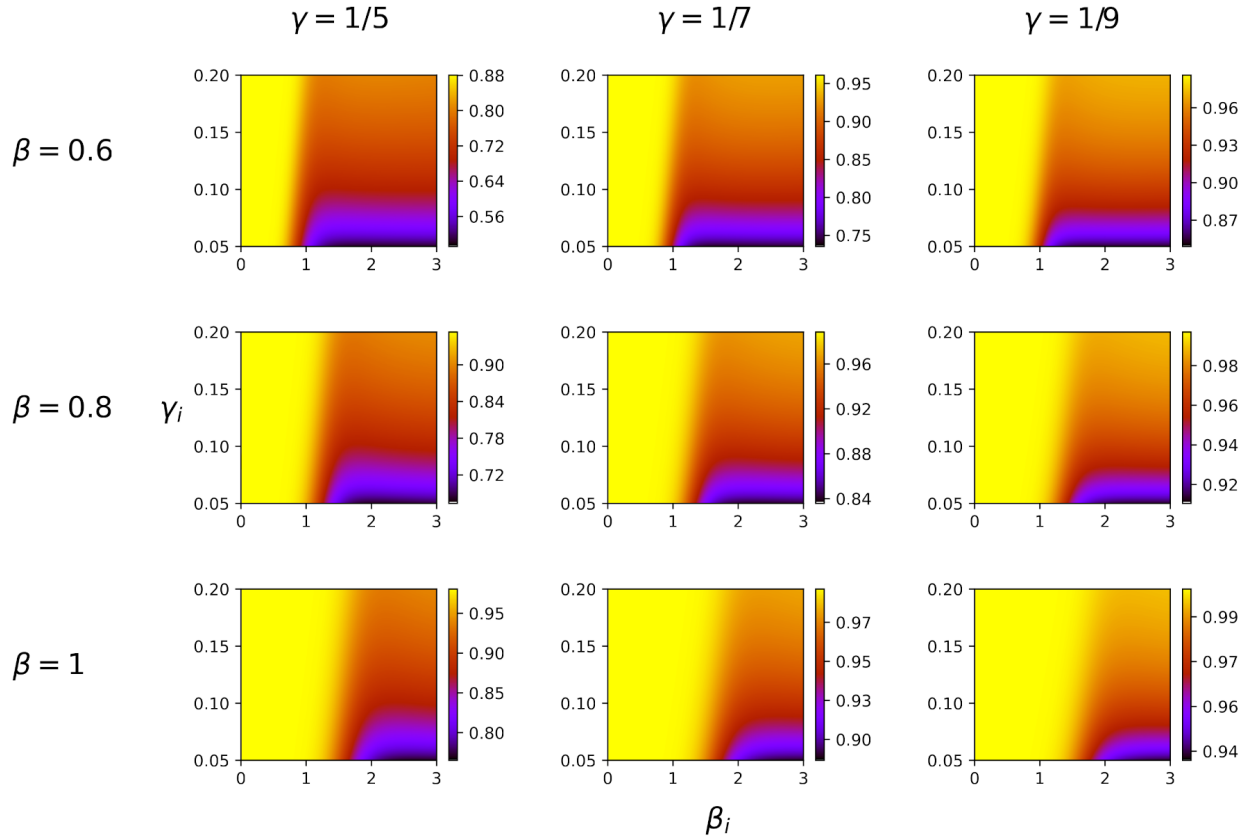


**Fig. S4: Grid of infectious parameters comparison in a multiple shot framework.** Shows the gradual change when different infectious and recovery rates are set in the infectious section of the model. Each subplot has its own color bar showing the distribution of values. The grid is composed by the sets of  $\beta \in \{0.6, 0.8, 1\}$  and  $\gamma \in \{1/5, 1/7, 1/9\}$ ; while the other parameters are considered fixed with  $\rho = 1/20$ .

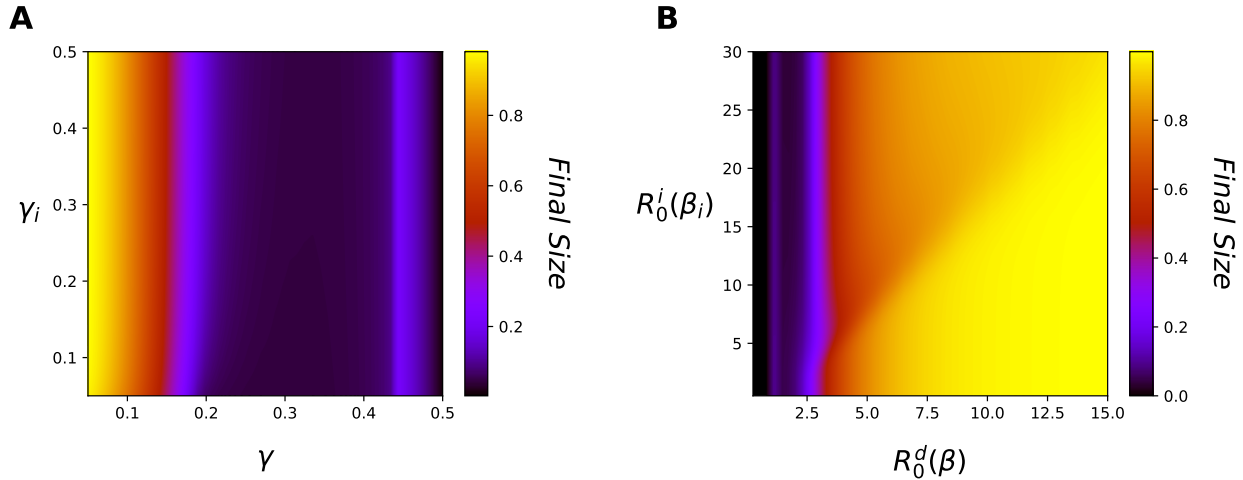


**Fig. S5: Comparison between rates of the same category in a single shot.** Contrast between behavioral and informational parameters represented with a heatmap, accompanied by a 3-dimensional perspective for better visualization. Recovery rates vary between  $[0.05, 0.5]$  while contagion rates vary between  $[0.05, 3]$ . The comparison of recovery rates is plotted in **(A)**. Similarly, the contagion rates are contrasted in **(B)**.

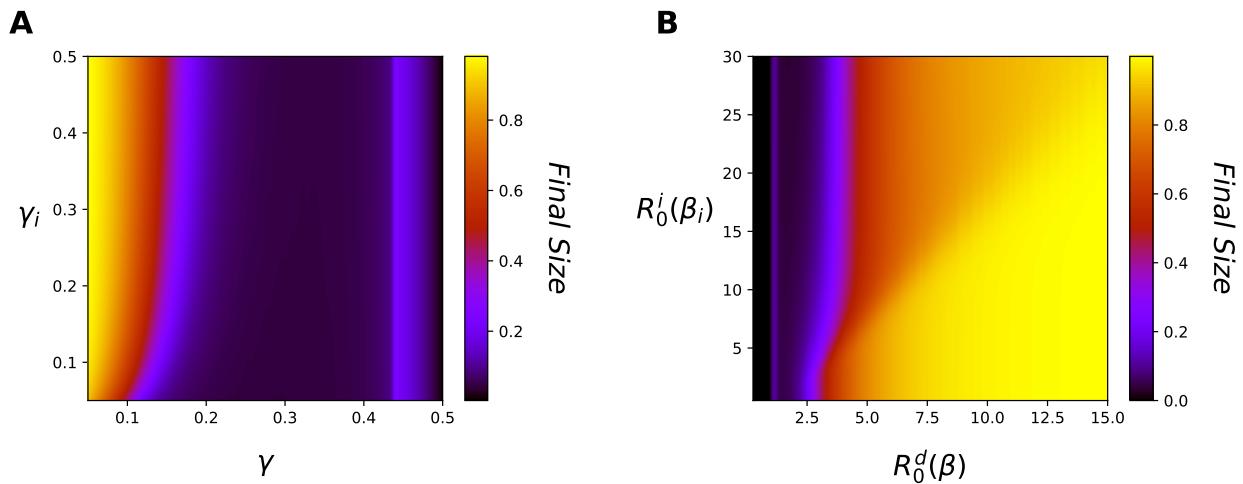


**Fig. S6: Comparison between rates of the same category in a multiple shot.** Contrast between behavioral and informational parameters represented with a heatmap, accompanied by a 3-dimensional perspective for better visualization. Recovery rates vary between  $[0.05, 0.5]$  while contagion rates vary between  $[0.05, 3]$ . The comparison of recovery rates is plotted in **(A)**. Similarly, the contagion rates are contrasted in **(B)**.

## Behavioral response with relapse scenario

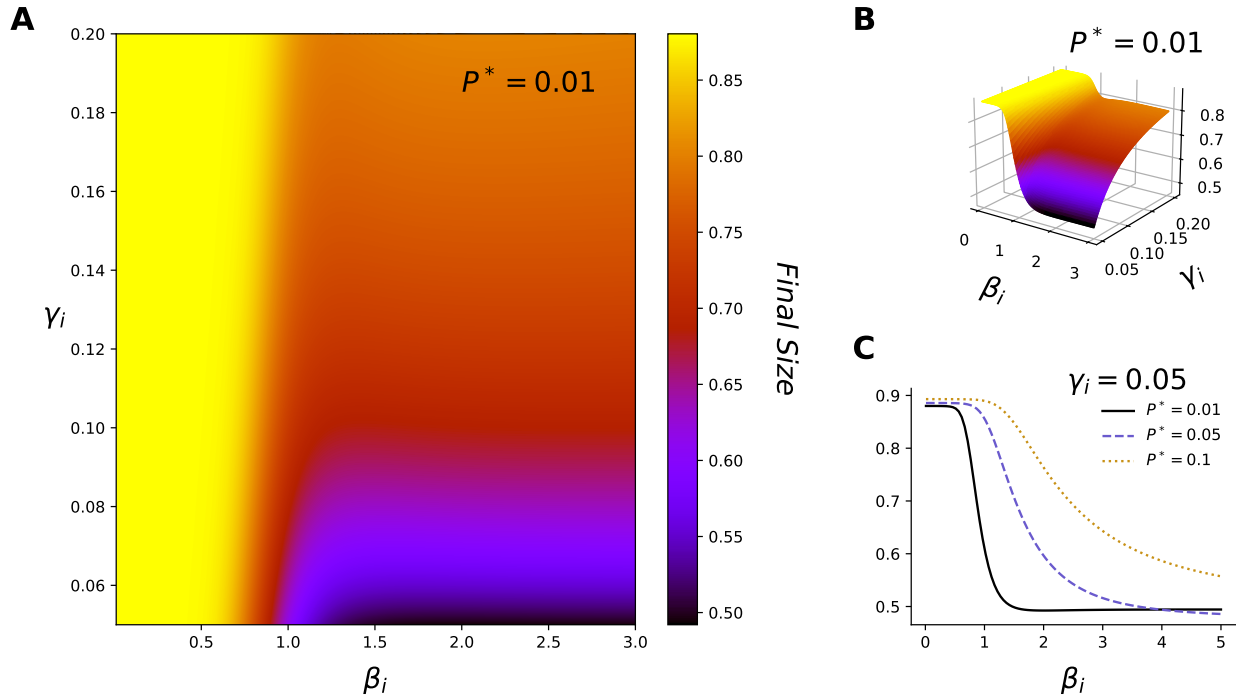


**Fig. S7: Impact of behavior in the epidemic final size based on comparison of informative parameters in a multiple shot framework.** (A) Heatmap of the epidemic final size based on the informative parameters. The parameter  $\beta_i$  varies between  $[0.01, 3]$  while  $\gamma_i$  varies between  $[0.05, 0.2]$ . The remaining parameters, which are kept fixed during the simulation, are  $\beta = 0.6$ ,  $\gamma = 0.2$ ,  $\epsilon = 0.8$ ,  $\phi = 0.2$ ,  $\rho = 1/20$  (multiple shot) and  $P = 0.01$ . (B) A 3-dimensional perspective of (A) with the same parameters, for better understanding. (C) Three simulations are done, with same parameters and  $\gamma_i = 0.05$ , for three distinct prevalence thresholds  $P = 0.01, 0.05, 0.1$ .

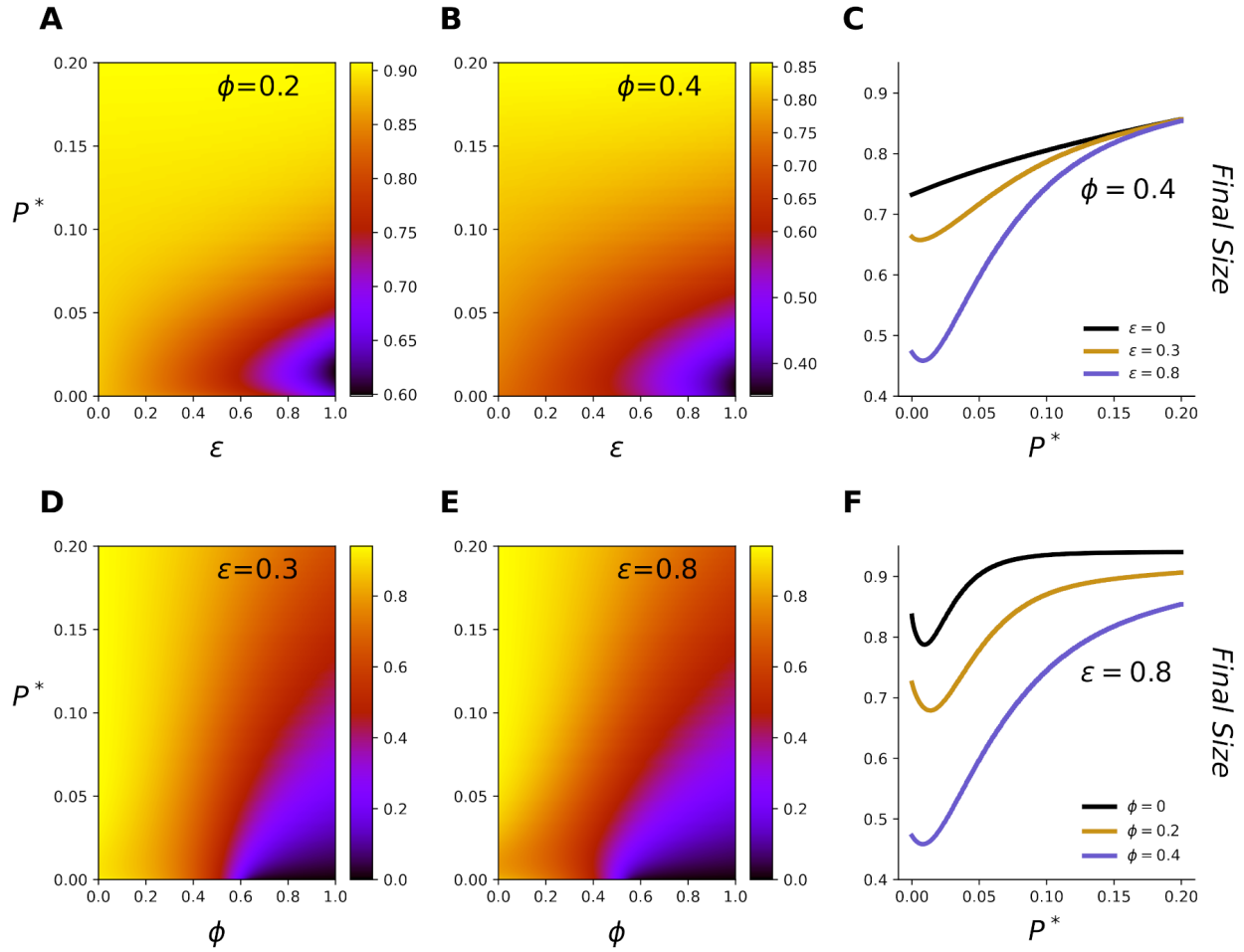


**Fig. S8: Change in epidemic final size by varying the prevalence threshold and behavioral parameters in a multiple shot framework. (A and B)** Different scenarios by modifying the parameter  $\phi = 0.2, 0.4$  respectively for (A) and (B) to get the epidemic final size, where  $\epsilon$  is varied between  $[0, 1]$  and  $P$  between  $[0, 1]$ , while keeping the rest of the parameters fixed,  $\rho = 1/20$  (multiple shot),  $\beta = 0.6$ ,  $\gamma = 0.2$ ,  $\beta_i = 1.5$  and  $\gamma_i = 0.1$ . **(D and E)** Images representing the same as in (A and B), with the difference being that the epidemic final size is obtained by varying  $\phi$  instead of  $\epsilon$ , and considering two cases for  $\epsilon = 0.3, 0.8$  respectively for (D and E). **(C and F)** Vertical trajectories obtained from (B and E) for (C and F) respectively.